Canalization of Phenotypes—When the Transcriptome is Constantly but Weakly Perturbed

Guang-An Lu,[†,1] Jinning Zhang,[†,1] Yixin Zhao [†,‡,1] Qingjian Chen [§,1] Pei Lin [¶,1] Tian Tang,[1] Zhixiong Tang,[1] Haijun Wen,[*,1] Zhongqi Liufu,[*,2] and Chung-I. Wu[*,1,3]

[1]State Key Laboratory of Biocontrol, School of Life Sciences, Southern Marine Science and Engineering Guangdong Laboratory (Zhuhai), Sun Yat-sen University, Guangzhou 510275, China

[2]Key Laboratory of Biological Targeting Diagnosis, Therapy and Rehabilitation of Guangdong Higher Education Institutes, The Fifth Affiliated Hospital of Guangzhou Medical University, Guangzhou 510799, China

[3]Department of Ecology and Evolution, The University of Chicago, Chicago, IL 60637

[†]These authors contributed equally to this work.

[‡]Present address: Simons Center for Quantitative Biology, Cold Spring Harbor Laboratory, Cold Spring Harbor, NY.

[§]Present address: State Key Laboratory of Oncogenes and Related Genes, Department of Oncology, Shanghai General Hospital, Shanghai Jiao Tong University School of Medicine, Shanghai, China.

[¶]Present address: The Shu Chien-Gene Lay Department of Bioengineering, University of California, San Diego, CA.

***Corresponding authors:** E-mails: wenhj5@mail.sysu.edu.cn; 2022687087@gzhmu.edu.cn; ciwu@uchicago.edu.

Associate editor: John True

Abstract

Recent studies have increasingly pointed to microRNAs (miRNAs) as the agent of gene regulatory network (GRN) stabilization as well as developmental canalization against constant but small environmental perturbations. To analyze mild perturbations, we construct a Dicer-1 knockdown line (*dcr-1* KD) in *Drosophila* that modestly reduces all miRNAs by, on average, ∼20%. The defining characteristic of stabilizers is that, when their capacity is compromised, GRNs do not change their short-term behaviors. Indeed, even with such broad reductions across all miRNAs, the changes in the transcriptome are very modest during development in stable environment. By comparison, broad knockdowns of other regulatory genes (esp. transcription factors) by the same method should lead to drastic changes in the GRNs. The consequence of destabilization may thus be in long-term development as postulated by the theory of canalization. Flies with modest miRNA reductions may gradually deviate from the developmental norm, resulting in late-stage failures such as shortened longevity. In the optimal culture condition, the survival to adulthood is indeed normal in the *dcr-1* KD line but, importantly, adult longevity is reduced by ∼90%. When flies are stressed by high temperature, *dcr-1* KD induces lethality earlier in late pupation and, as the perturbations are shifted earlier, the affected stages are shifted correspondingly. Hence, in late stages of development with deviations piling up, GRN would be increasingly in need of stabilization. In conclusion, miRNAs appear to be a solution to weak but constant environmental perturbations.

Key words: **cannalization, gene regulatory network, microRNA.**

Article

Introduction

Living organisms face internal and external fluctuations constantly. These fluctuations would broadly perturb many phenotypes. Hence, the maintenance of stable phenotypic output and normal development under such perturbations is an important topic as emphasized by Waddington (1942, 1959). He coined the term "developmental canalization" for the development along a defined path. A standard depiction is a ball traveling along a canal in a landscape of many canals, each for a tissue of a particular species (Waddington 1957; Scharloo 1991).

There are two approaches to observing developmental canalization. The first one is to measure the variance of phenotypic values at a particular stage of development. Such measurements of phenotypic robustness have been frequently adopted in the literature (Levy and Siegal 2008; Kasper et al. 2017; Hintze et al. 2021), and reviews (Rendel 1967; Félix and Barkoulas 2015; Takahashi 2019). A second approach, taken in this study, is to follow the development to the final stages (i.e., maturation to adulthood and death) as Waddington envisaged (Wagner 2005). Decanalization will be observed as increasingly aberrant phenotypes as development progresses.

Molecular biology and mathematical theories of developmental canalization have been proposed (Wagner 2005; Siegal and Leu 2014; Saiz et al. 2020). Although the concept of canalization is developed to account for the phenotypic stability, the effect can be more easily studied at the level of the gene regulatory network (GRN; Chen et al. 2019; Guo and Amir 2021). After all, phenotypic changes are

downstream of GRN variations. At the molecular level, several genes (Hallgrimsson et al. 2019), including Hsp 90 (Rutherford and Lindquist 1998), have been proposed to have the canalizing capacity.

Most notable, a general class of genes that may play a crucial role in canalization has been proposed to be the microRNAs (miRNAs; Wu et al. 2009; Posadas and Carthew 2014). According to the annotations in miRBase (Kozomara et al. 2019), each metazoan species often has hundreds of miRNAs and many of them are expressed in most cells (Ludwig et al. 2016; Zhao et al. 2018; Rahmanian et al. 2019). Each miRNA of ~21 nt in size could weakly but broadly repress hundreds of target genes post transcription (Bartel 2018). The diffuse (i.e., weak but broad) and uni-directional (downward) regulation is the unique feature of miRNAs (Farh et al. 2005). This mode of regulation has led to the demonstration of incoherent regulation (Liufu et al. 2017) and the mathematical formulation of GRN canalization by miRNAs (Zhao et al. 2017; Chen et al. 2019).

In testing the hypothesis of miRNA canalization, miRNAs collectively are regarded as a single regulatory unit. We then reduce the entire miRNA pool modestly and evenly by creating a *dcr-1* KD line (for Dicer knockdown). In this *dcr-1* KD background, several expectations can be formulated. First, at the molecular level, *dcr-1* KD should have only marginal effects on transcriptome under normal condition, this being the main characteristic of GRN stabilizers. The consequences of *dcr-1* KD would be detectable only under stresses or in long-term development. Second, fly development would deviate gradually from the set course as the development progresses. Third, the deviation would be hastened by environmental stresses including temperature aberrations. Our study will test if these expectations are fulfilled.

Results

This section is organized around the central hypothesis that 1) miRNAs collectively stabilize the GRN in the face of constant (but often modest) perturbations; and 2) the stabilizing effect ensures the proper execution of development from embryogenesis to adulthood. Stabilizers are distinct from other regulatory mechanisms in a unique way: The removal of GRN stabilizers would not by itself perturb the GRN. Hence, in the absence of strong external perturbations, removing the stabilizers would not have much immediate consequence. However, over a long period, especially in later stages of development with the cumulative small perturbations, the development may gradually come to a halt.

To test the main hypothesis, instead of removing specific miRNAs completely, we reduce all miRNAs modestly (by 15–25%) in Part I. In doing so, we reduce the stabilizing capacity while minimizing the perturbations. In Part II, we test the first aspect of the hypothesis that the reduction in miRNAs would not perturb the transcriptome strongly in the absence of external perturbations. In Part III, we compare the effect of miRNA reductions on the GRN with the similar treatments of transcription factors (TFs), another major class of expression regulators. As miRNAs are stabilizers, the reduction in their capacity should not directly affect the transcriptome in the absence of perturbation. (The analogy is that lifting the hands off the steering wheel on a straight road would still keep the vehicle on course, at least for a while.) In contrast, TFs should have direct impacts on the transcriptome; hence, TFs are true expression regulators and miRNAs are not. A detailed exploration of the mathematics of miRNAs versus TFs has been presented in Chen et al. (2019) in an extension of the May–Wigner theory.

Part IV tests the second aspect of the central hypothesis. As the organism develops, the development may gradually come to a halt with the accumulations of perturbations that are not corrected. The development fails even though short-term measurements of gene expression in earlier stages seem normal.

Part I—Reduction of Total miRNAs by *dcr-1* KD

In Part I, we reduced the amount of all miRNAs by knocking down the Dicer-1 gene (*dcr-1* KD). Although knocking down the entire biosynthesis is not commonly done for its potential severity, it can be effective under some circumstances (e.g., Wen et al. 2021). Note that knockdown is a far milder treatment than knockout. As a result, miRNAs would be reduced moderately and the expressions of their target genes should only be marginally affected. After all, even miRNA knockout would result in the changes in the expression by ~10%, when averaged over all inferred targets. (For the various definitions of miRNA targets, please refer to Zhao et al. 2017, 2019, and Seitz 2019; and debates in *Molecular Biology and Evolution*.) We used a weakly and broadly expressed Gal4 construct (Hrdlicka et al. 2002) to drive the interfering RNA that knocks down *dcr-1* (Ni et al. 2011). In reverse transcription-quantitative polymerase chain reaction (RT-qPCR), the observed *dcr-1* expression decreases modestly by 25–30% (Student's *t*-test, $P < 0.05$; fig. 1*A*).

As a consequence of the Dicer-1 knockdown, most miRNAs are slightly down-regulated, usually in the range of 15–25% (fig. 1*B* and supplementary fig. S1, Supplementary Material online). Figure 1*C* presents the expression differences of individual miRNAs in the *dcr-1* KD background. These selected miRNAs range from being highly to lowly expressed and the level of reduction appears even across the board. These results show that the measurements of miRNA abundance correlate well with the dicer expression between sexes and between temperature treatments. Furthermore, our previous publication (Ma et al. 2020) has confirmed the global impact of Dicer inhibition on miRNAs in this background (*T98-Gal4/+*; *UAS-Dicer-1*^{HMS00141}*/+*) by high-throughput small RNA-seq. When using the reads of piRNA for data normalization, the expression of miRNAs showed significantly and broadly down-regulation in the *dcr-1* KD

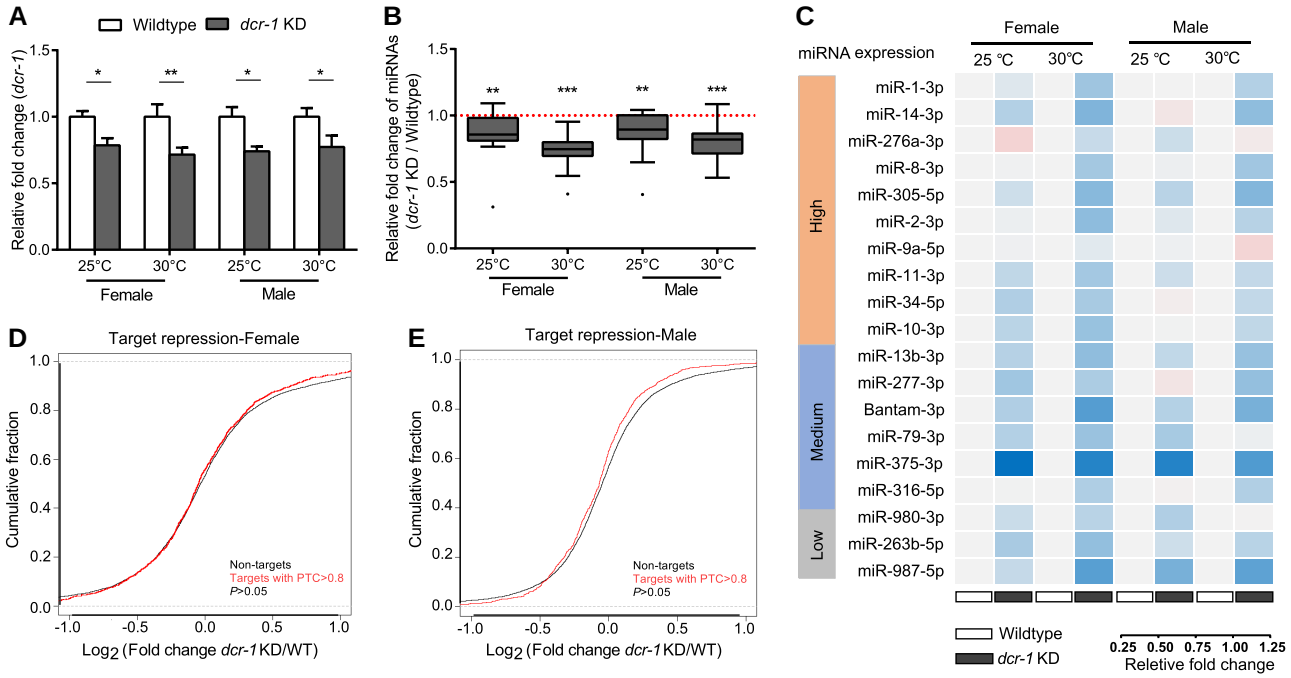

Fig. 1. *dcr-1* KD leads weak but broadly reduction in miRNA pool. (*A*) Impact of RNAi on *dcr-1* expression. Bar plots show the mean with SD for the relative expression of *dcr-1* in female and male L3 with different genotypes at two temperatures. For both sex and temperature, *dcr-1* expression significantly decreases 25–30% in *dcr-1* KD larvae. (Two-tail Student's *t*-test, $^{*}P < 0.05$, $^{**}P < 0.01$.) (*B* and *C*) Impact of *dcr-1* RNAi on miRNA expression. (*B*) Summary of relative fold change of 19 selected miRNAs, accounting for over 50% of the total sequencing reads in the L3 (for more details, see supplementary fig. S1, Supplementary Material online). These miRNAs are down-regulated modestly but broadly at both 25 and 30 °C, one sample *t*-tests are performed to test whether the up-regulation is significantly deviates from 1, $^{**}P < 0.01$, $^{***}P < 0.001$. (*C*) Heat map shows relative expression of selected miRNAs in female and male L3 with different genotypes at two temperatures. Relative expression levels of miRNAs in wildtype flies are set to 1. (*D* and *E*) Impact of *dcr-1* RNAi on miRNA targets in female (*D*) and male (*E*) transcriptomes. Conserved miRNA targets (TargetScan PTC > 0.8) do not show significant change compared with non-targets ($P > 0.05$, Kolmogorov–Smirnov test). QRT-PCR is performed in triplicate for genes and miRNAs, *rp49* and *U6* are used as inner reference controls for genes and miRNAs, respectively. Genotype: Wildtype (*T98-Gal4/+*; *UAS-GFP/+*); *dcr-1* KD (*T98-Gal4/+*; *UAS-Dicer-1* ^{HMS00141}*/+*).

background (Ma et al. 2020, supplementary fig. S3, Supplementary Material online). Because the complete knockout of each miRNA would generally increase the target gene expression by <50%, the partial knockdown is expected to have rather mild effects on these expression levels of figure 1*D* and *E* corroborate the expectation. For the impact of miRNA KD on target gene expression, we do not expect significant differences between the dicer-KD line and the wildtype. To begin with, given only 20% reduction in each miRNA, the effects on the direct targets, conserved or unconserved, are quite small. Importantly, when all miRNAs are weakly knocked down, all genes are indirect targets of some miRNAs as the actual targeting miRNAs are in the minority. As a result, there are numerous compensatory repressions and derepressions, often leading back to the original expression levels. Figure 1 panels collectively show that *dcr-1* KD exerts weak but broad perturbations on the transcriptome.

Part II—Changes in the GRN of *dcr-1* KD Lines

The selection of tissues and developmental stages for the analysis of GRNs in the *dcr-1* KD lines is based on a hypothesis. We posit that, in the developmental stages when the phenotype is still normal but is at the cusp of imminent changes, the underlying transcriptome should have already shown some deviations from the norm. We hence examine the transcriptome right before phenotypic abnormalities become observable, that is, the late third instar larvae (L3).

The analysis of figure 2*A* (orange squares) shows that the transcriptome in *dcr-1* KD appears normal in different temperatures and in both sexes. This observation corroborates the expected behaviors of the GRN stabilizers which do not exert their effects in the absence of perturbation. In figure 2*A*, the correlation coefficients are organized in three tiers—wildtype versus *dcr-1* KD (orange), 25 versus 30 °C (green) and male versus females (blue). In the comparisons, we observed sex to have the largest impact (coefficient ranging from 0.841 to 0.879), whereas the temperature effect is relatively modest (coefficient ranging from 0.976 to 0.984 and 0.938 to 0.978 for male and female, respectively). Most interesting, *dcr-1* KD has very little effect (between 0.975 and 0.988) on the transcription patterns. Further statistical analysis by a general linear model (Materials and Methods) reveals 56%, 32%, and 9% of the genes are significantly affected by sex, temperature, and *dcr-1* KD, respectively (supplementary fig. S2,

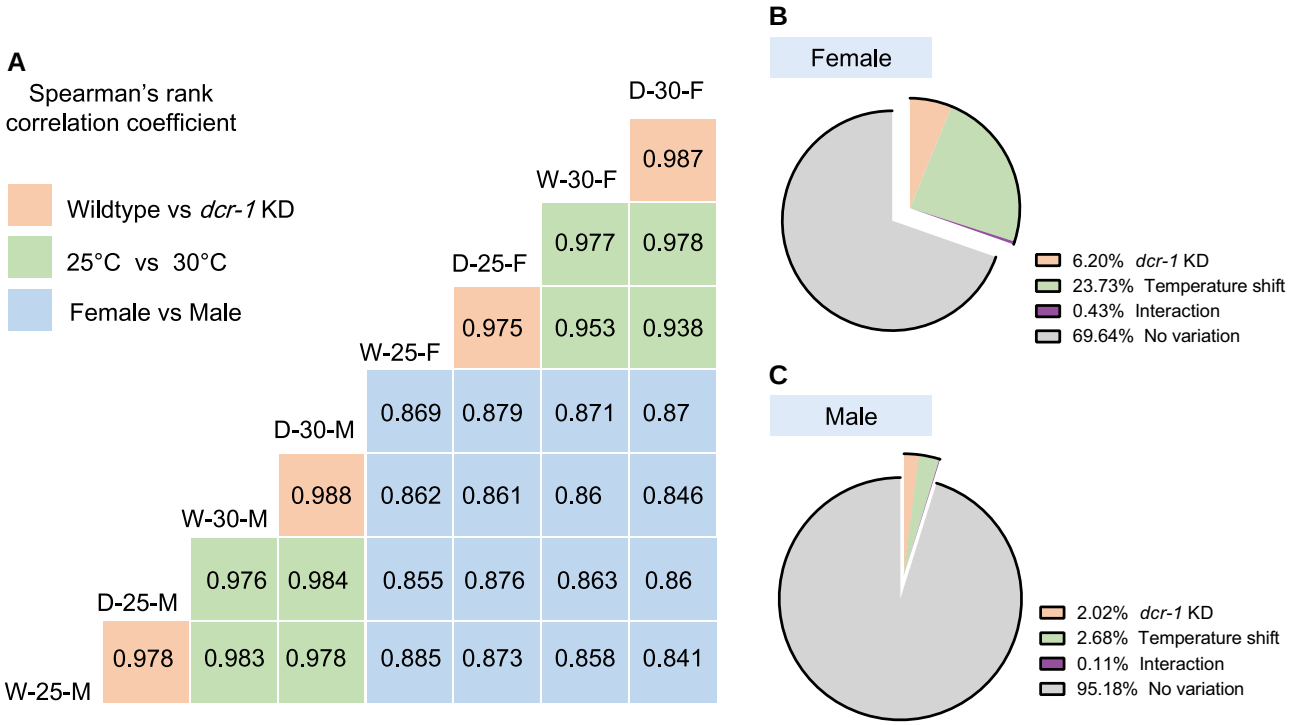

Fig. 2. *dcr-1* KD results in "normal" but wobbly transcriptome. (*A*) Pairwise correlations among whole transcriptomes in RNA-seq data sets. RNA-seq data was generated for each sex (female and male) × genotype (Wildtype and *dcr-1* KD) × temperature (25 and 30 °C) combination for L3. Correlations fall into three tiers, reflecting the impact of sex (Female versus Male), temperature (25 °C versus 30 °C), and *dcr-1* KD (wildtype versus *dcr*-1 KD), respectively. (*B* and *C*) Impact of temperature, *dcr-1* KD and their interaction on gene expression profiles for females (*B*) and males (*C*). The pie plot shows the percentage of genes affected by *dcr-1* KD, temperature shifts, genotype × environment interactions and no variation according to a generalized lineal model method (see Materials and Methods).

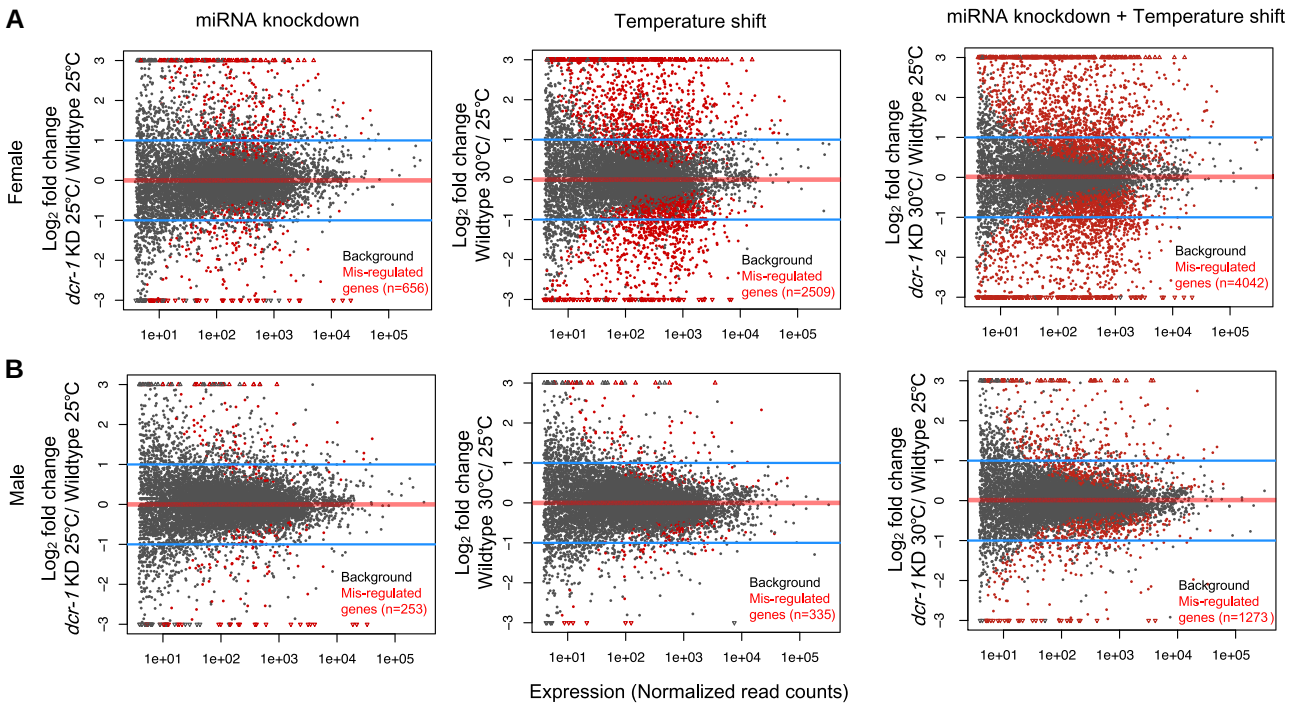

Fig. 3. Dysregulated genes in the *dcr-1* KD lines. (*A* and *B*) Significantly dysregulated genes affected by three types of perturbation for females (*A*) and males (*B*). Genes affected by *dcr-1* KD, temperature shift and both are plotted in left, middle and right panel, respectively. Gray dots show all genes expressed in L3, whereas red dots show the significantly dysregulated genes detected by DEseq2 with FDR < 0.1.

Supplementary Material online). When dividing sex and adding the interactions into the general linear model (Materials and Methods), we observed the consistent pattern that *dcr-1* KD has a smaller effect on the transcriptome compared with temperature shift (fig. 2*B* and *C*). These results support the conjecture of a normal transcriptome in *dcr-1* KD in the absence of perturbation.

The results of figure 2*A*–*C* are about the overall expression patterns under various conditions. With the stabilization mechanism compromised, we expect some genes to deviate from the norm in expression, even though the mean expression appears unchanged. These outlier expressions will be an indication of reduced GRN stability under the influence of a smaller miRNA pool. In these experiments, we compared the number of dysregulated genes under three different comparisons: *dcr-1* KD, temperature shift and both.

Although figure 2 is about the overall expression patterns, figure 3 examines the expression deviations in individual genes. In the first panel of figure 3, we observe the overall dispersion of gene expression in the *dcr-1* KD background with little bias in either up- or down-regulation. Such deviations can be interpreted as expression instability, rather than directional expression dysregulation. Again, although *dcr-1* KD has much less impact on the transcriptome than temperature shift, *dcr-1* KD exacerbates the stress of temperature shift on the transcriptome, resulting in more dysregulated genes (fig. 3) in various gene ontologies (supplementary table S1, Supplementary Material online). In conclusion, GRN becomes less stable with more dysregulated genes when miRNAs are modestly reduced across the board.

Part III—GRN Changes in TF Knockdown vs. miRNA Knockdown Lines

Part II shows that, when miRNAs are broadly knocked down, the transcriptome are only slightly perturbed with the Pearson's *r* ranging between 0.97 and 0.99. Note that the higher the *r*-value, the smaller the effect of the gene knockdown. To see how small (and also how unusual) the miRNA effects are, we use the knockdown effects of TFs for a comparison. Public RNA-seq data of RNAi-mediated knockdown of each of many TFs are available for *Drosophila* S2 cells (References GSE89753). As our experiments of miRNA knockdown are also based on RNA-i, the comparison should be valid.

We choose one TF from each of the 18 TF gene families (see Materials and Methods for the selection). Table 1 presents the correlation coefficient (Pearson's *r*) between the transcriptomes of TF KD lines and the wildtype control. Roughly, one-third of the TF KD lines has a high *r*-value (>0.98) and another one-third has a moderately high *r* between 0.92 and 0.97. The remaining one-third has a lower and variable *r*-value, spread between 0.48 and 0.90.

Since the miRNA KD line has a partial expression reduction of *all* miRNAs, a proper comparison should be a similar partial reduction of all TFs. Unfortunately, although such experimentation is feasible for miRNAs via dicer-KD, it cannot be done for TFs. One may nevertheless assume that a broad knockdown of TFs should be at least as severe as some of the most severe effects of the individual TF-KD lines, whereby the Pearson's *r* ranges between 0.48 and 0.72. In this comparison, the effect of miRNA knockdown on the transcriptome indeed appears far weaker than that of TF knockdowns.

Although it is not possible to determine the effect of broad TF knockdown on the GRN by experimentation, we may make an inference of the TF effect by computational means. In Materials and Methods, we describe the inference on the assumption that multiple TF affect the gene expression multiplicatively. The cumulative effect of multiple genes may or may not be more severe than the effect of individual TFs because nearly half of the TFs upregulate and the other half down-regulate their targets. Hence, it seems plausible that broad and mild knockdowns of TFs may not perturb the GRN strongly. However, as presented in table 1, the computationally inferred effect yields

Table 1. Effect of TF Versus miRNA Knockdown on the Transcriptome and Development.

Single transcription factors			
TF Family	**Gene**	**Pearson's *r*[a]**	**Stage of phenotypic defect[b]**
TALE/PBX Homeobox	*exd*	0.9901	I
p53	*p53*	0.9895	V
HSF	*Hsf*	0.9888	II
TEA/ATTS	*sd*	0.9881	II
NHR ZF	*Hr39*	0.9868	III
LIM Homeobox	*ap*	0.9858	III
SAP	*Mrtf*	0.9696	II
GATA ZF	*pnr*	0.9525	I
SANT/Myb	*Myb*	0.9442	II
MEF2	*Mef2*	0.9333	I
bHLH	*da*	0.9322	I
WD repeat mio	*Mio*	0.9255	IV
Zeste	*z*	0.8913	V
C2H2 ZF	*zfh1*	0.8736	I
ETS	*pnt*	0.711	I
bZIP	*kay*	0.6983	I
E2F/DP	*E2f1*	0.6705	II
CUT Homeobox	*ct*	0.4838	I
Aggregate effect of the 18 TF knockdowns (estimated)[c]		**0.0313**	
Aggregate effect of all miRNA knockdowns via Dicer-KD			
25 °C-Female		**0.9735**	**V**
25 °C-Male		**0.9780**	**V**
30 °C-Female		**0.9876**	**III**
30 °C-Male		**0.9884**	**III**

NOTE.—The TF family is based on the UniProt/InerPro evidence.
[a]Correlation between the gene expression profile of the wildtype fly and that of the TF (or miRNA) knockdown lines (see the main text for detail).
[b]For TF, the loss-of-function phenotype reported in FlyBase is used. I, embryonic lethal; II, larval lethal; III, pupal lethal; IV, abnormal adult –sterile or unable to survive to adulthood; V, sub-normal adult—viable and fertile adults with aberrant phenotypes.
[c]Correlation between the genes expression of wildtype and the estimated expression of the "aggregate" TF knockdowns of the 18 genes. In the aggregate, the expression of each gene (y) is calculated as:
$y = \log_{10}$ WT + $\log_{10}$ (Fold change TF-1 KD/WT) + $\log_{10}$ (Fold change TF-2 KD/WT) +…+ $\log_{10}$ (Fold change TF-18 KD/WT).

a very low Pearson's *r* of only 0.0313. In other words, the inferred GRN under multiple TF knockdowns is almost entirely uncorrelated with the wildtype. Most important, this pattern is very divergent from the miRNA effect.

Table 1 also presents the effect of TF KD on development. There is indeed a trend that the developmental effect is more severe when the deviation from the control is greater (supplementary fig. S3, Supplementary Material online). However, the correlation is rather weak as many TF KD lines show early developmental defects, whereas the transcriptome appears almost fully normal. It is likely that the TF KD only perturbs a very small number of crucial genes. In the next section, we will present the developmental effects of dicer-KD lines which again distinguish miRNA effects from those of TFs.

Part IV—Developmental Effects of *dcr-1* KD

In this last part, we present the measurements of phenotypic effects in dcr-1 KD lines. Part II has shown that the transcriptomic changes by the treatment are rather weak, especially in comparison with the knockdown of TFs.

Phenotypic Consequence of dcr-1 KD Under Standard Culture Conditions

During the development, GRNs are constantly perturbed. With the canalization by miRNAs weakened, the consequence is expected to be cumulative, affecting the late stages of development severely. We therefore measured the life-history traits (fig. 4A) across the developmental stages (egg hatchability, larval viability, pupal viability, and adult longevity) expecting normal development in the early stages but uncertainties in late ones.

Under standard conditions at 25 °C, *dcr-1* KD flies indeed develop normally showing little adverse effects in egg hatchability, larvae viability, and pupation. Strikingly, toward the very end of the development, adults experience 80% reduction in longevity in both sexes (one-way analysis of variance [ANOVA], $P < 0.05$; fig. 4B). The phenotypic defect in lifespan could be rescued by reintroducing UAS-*dcr-1* into the *dcr-1* KD background (Materials and Methods, supplementary fig. S4, Supplementary Material online). The occurrence in the *dcr-1* KD flies of defects only in the late developmental stages is consistent with the hypothesis of miRNAs role in developmental canalization.

Phenotypic Consequences of dcr-1 KD Under High Temperature

We then explored if miRNA can ameliorate the perturbation of temperature shift from the standard 25 to 30 °C. The higher temperature, known to be stressful to the flies (Chen et al. 2015; Sgro et al. 2016; Vihervaara et al. 2018), should not be uncommon in nature. In the *dcr-1* KD background, the perturbation happens in flies with the stability control compromised, analogous to a high-wire walker without the pole.

Growing in 30 °C, *dcr-1* KD flies displayed severe phenotypic defects with >95% decrease in both pupal viability and adult longevity (fig. 4C and D). Hence, the defects are much more severe than in 25 °C. Most flies cannot complete the normal development which could be stalled in various pupal stages (supplementary fig. S5, Supplementary Material online). Since the failure to develop does not happen in a defined stage, the observation again suggests some cumulative effects in the miRNA KD background. In short, even though fly development is well canalized, the modest miRNA knockdown still leads compromised stabilization (fig. 4D). In all experiments, the rescue line is also used. Although the rescue can usually be observed, it may at times be rather weak under extreme conditions as in figure 4D. We will discuss this incomplete rescue in Discussion.

Phenotypic Consequence of dcr-1 KD Under Transient High-Temperature Shift

The cumulative effect of miRNA KD on development can be best demonstrated with transient temperature shift. The temperature is raised to 30 °C in either a 24- or 72-h pulse (fig. 5A). We found *dcr-1* KD could significantly decrease fly fitness by all heat pulses (fig. 5B and C; one-way ANOVA, overall $P < 0.05$).

For females, *dcr-1* KD flies reflect significant decreases in both pupal viability and lifespan after transient temperature shift. We observed that as the perturbations are shifted earlier (larvae vs. pupae or adults), the affected stages are shifted correspondingly, leading to more severe decrease in both viability and longevity (fig. 5B and C, up panel). We also found that these fitness decreases reveal cumulative effect as a function of developmental progression (fig. 5B and C, up panel), with stronger effects toward the late developmental stages (adults). For males, *dcr-1* KD flies also show significantly decreases in lifespan after transient temperature shift (fig. 5B and C, down panel). As for the sex differences in the phenotypes of *dcr-1* KD, we suggest that the differences may simply be a "Tail end" effect (a small difference in mean becoming a large difference in the tail of the distribution) reflecting the innate sexual difference. Collectively, these results suggest that the pronounced phenotypes of *dcr-1* KD at 30 °C represent the cumulative effects of perturbations through development.

Discussion

In 1942, Waddington proposed that "developmental reactions…bring about one definite end-result regardless of minor variations" (Waddington 1942). This statement is the genesis of the canalization view. Since then, the genetic circuitry required for canalization has been a constant topic. The view on canalization in recent years has been extended from the analysis of small-scale circuits (Ebert and Sharp 2012; Siciliano et al. 2013), to modules (Peláez and Carthew 2012), and then to large-scale regulatory networks (Ambros 2019; Chen et al. 2019). In particular, Chen et al. (2019) adopted the May–Wigner theory

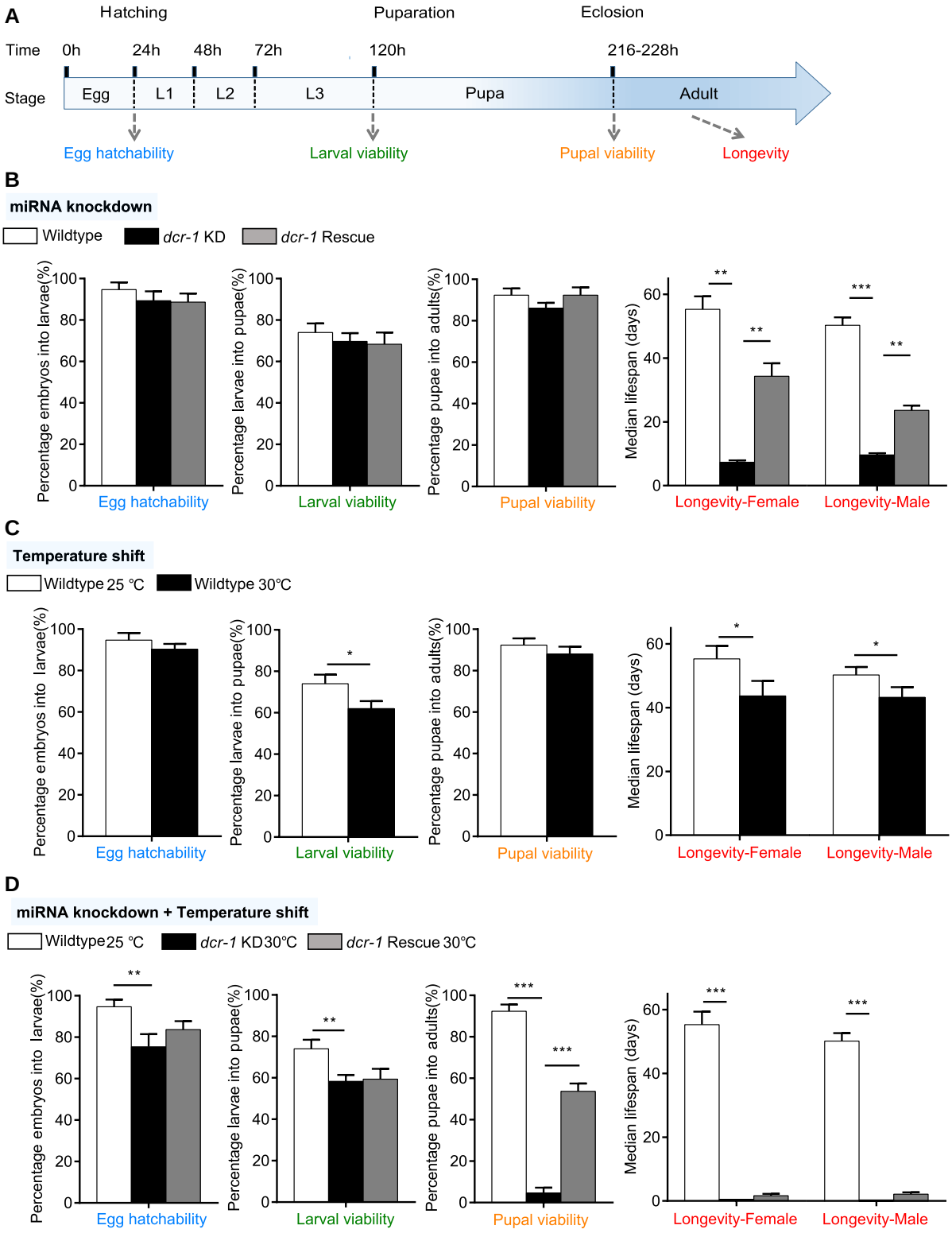

Fig. 4. Phenotypic consequences of *dcr-1* KD under standard and high temperature. (*A*) Experimental design for fitness component assays (indicated by arrows) across the whole *Drosophila* developmental process. Four typical fitness components (egg hatchability, larval viability, pupal viability, and adult longevity are measured. (*B*) Phenotypic consequences of miRNA knockdown. Compared with wildtype, *dcr-1* KD files reveal no significant changes in egg hatchability, larval or pupal viability, whereas strikingly decrease longevity at 25 °C. This phenotypic defect can be partially rescued by co-expressing *UAS-dcr-1* in the rescue line (one-way ANOVA with Tukey correction for multiple comparisons, $^{**}P < 0.01$, $^{***}P < 0.001$). (*C*) Phenotypic consequences of temperature shift. High temperature slightly reduces these fitness components. Student's *t*-test is used for significance tests, $^{*}P < 0.05$. (*D*) Phenotypic consequences of both temperature shift and miRNA knockdown. *dcr-1* KD flies reveal striking decreases in pupal viability and longevity at 30 °C. These phenotypic defects can be partially rescued in the rescue flies (one-way ANOVA with Tukey correction for multiple comparisons, $^{*}P < 0.05$, $^{**}P < 0.01$, $^{***}P < 0.001$). Genotype: Wildtype (*T98-Gal4/+*; *UAS-GFP/+*); *dcr-1* KD (*T98-Gal4/+*; *UAS-Dicer-1*^{HMS00141}*/+*); *dcr-1* rescue (*T98-Gal4/+*; *UAS-Dicer-1* ^{HMS00141}*/UAS-Dicer-1*).

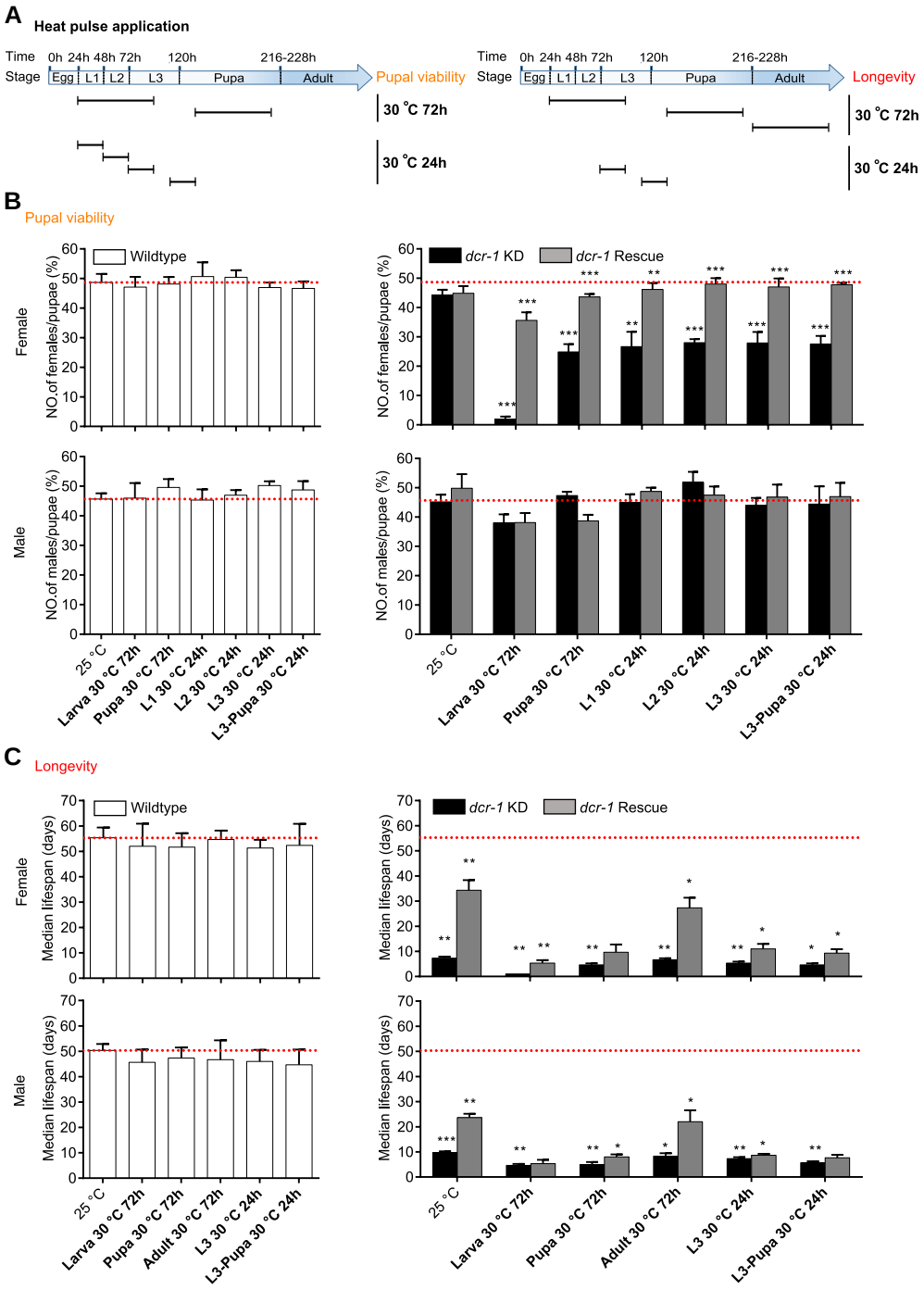

Fig. 5. Phenotypic consequences of *dcr-1* KD after transient temperature shifts. (*A*) Experimental design of the transient temperature shift (heat pulse) assay. Segment lengths indicate heat pulse durations (72 or 24 h). Two typical fitness components, pupal viability and longevity, are measured. (*B*) Pupal viability of wildtype, *dcr-1* KD and *dcr-1* rescue flies after different transient temperature shifts. Left panel, pupal viability of wildtype flies under different heat pulse assays. Right panel, pupal viability of *dcr-1* KD and *dcr-1* rescue flies under different heat pulse assays. The red line indicates the wildtype value without perturbation. After different heat pulse assays, pupal viability of wildtype flies decreased slightly, whereas pupal viability of *dcr-1* KD flies decreased significantly, especially in females. The phenotypic defect overall can be partially rescued in the rescue flies. Note that larval stages of *dcr-1* KD female flies are more sensitive to heat pulses (reduce to ~1.9% whereas others were around 26% compared with wildtype) and show cumulative effect (27% (L1 24 h HP) × 28% (L2 24 h HP) × 28% (L3 24 h HP) = 2.1%, which is nearly the same proportion, 1.9% with larva 72 h HP) of the lethality (one-way ANOVA with Tukey correct for multiple comparisons is performed, $^{**}P < 0.01$, $^{***}P < 0.001$). (*C*) Longevity of wildtype, *dcr-1* KD and *dcr-1* rescue flies. After different heat pulse assays, lifespan of wildtype flies decreased slightly, whereas lifespan of *dcr-1* KD flies decreased significantly. The phenotypic defect can be partially rescued in the rescue flies. For *dcr-1* KD flies, 72 h heat pulse at the larval stage has the strongest effect in both sexes. Note that *dcr-1* KD females are more sensitive to heat pulses than males (one-way ANOVA with Tukey correction for multiple comparisons, $^{*}P < 0.05$, $^{**}P < 0.01$, $^{***}P < 0.001$).

(May 1972, 1974) on the stability of complex systems to show how miRNA actions can stabilize GRNs.

The hypothesis can be schematically presented as: miRNA actions → GRN stability → developmental canalization. Although the first stage of "miRNA actions → GRN stability" is supported by a series of studies (Zhao et al. 2017; Chen et al. 2019), the influence of miRNAs on developmental canalization has only been indirectly inferred. For example, Chen et al. (2019) suggest that, without the GRN stability governed by miRNAs, developmental canalization might be untenable. An experimental attempt at proving this connection has been reported by Liufu et al. (2017) that the same miRNA may regulate the same developmental phenotype via multiple target genes, sometimes in the same but often in opposite directions. These antagonizing actions strongly hint, but do not prove, the role of miRNAs on developmental canalization.

In this study, the connections from miRNA to development via multiple links (i.e., miRNA actions → GRN stability → developmental canalization) are established. Furthermore, although previous reports (Li et al. 2009; Cassidy et al. 2013; Kasper et al. 2017), including (Liufu et al. 2017), analyze only a few chosen miRNAs, this study is based on the entire collection of miRNAs. It hence provides the first empirical evidence supporting the theoretical prediction that miRNAs collectively serve as the canalization agent of development. Given that the environment fluctuates constantly, but often mildly, our results show how development may cope with such most common perturbations.

Since first discovered in 1990s (Lee et al. 1993), miRNAs have been proposed to function in diverse biological processes (Bartel 2018). For example, previous studies have shown that miRNAs serve as molecular switches in cell differentiation (Nagosa et al. 2017; Galagali and Kim 2020) and developmental transitions (Jiang et al. 2014; Ambros and Ruvkun 2018) by repressing target genes (Eichhorn et al. 2014). Recent works have proposed that miRNAs work on gene circuits by reducing the expression noise of their targets, especially on the lowly expressed ones (Schmiedel et al. 2015; Wei et al. 2021). Furthermore, in our series works, we have emphasized repeatedly that miRNAs are unique among regulatory genes as their main function is to stabilize the expressions (Wu et al. 2009; Liufu et al. 2017; Zhao et al. 2017; Chen et al. 2019), whereas others are about changing the expressions or selective values (Chen et al. 2022). In this context, if other regulatory genes (e.g., a collection of TFs) are weakly and broadly reduced as was done here on miRNAs, we expect the transcriptome to be severely perturbed and development to be arrested quite early (table 1).

In the field of evolutionary genetics, miRNAs stand as a most dynamic class of genes with its high birth and death rate (Lu et al. 2008, 2018; Nozawa et al. 2012; Lyu et al. 2014; Zhao et al. 2021). The changing evolvability of miRNA targets indicated that miRNA's regulation contribute to the evolution of organismal diversity (Xu et al. 2013). In a companion study on the evolution of gene expression under miRNAs (Lin et al. 2022) extends the connections in time scale from short-term development to long-term evolution, schematically represented as miRNA actions → GRN stability → developmental canalization → evolution. By showing the continual gains and losses of miRNA target sites during evolution, they suggest that miRNAs keep the target gene expressions near an optimal level, until the optimum shifts occasionally during long-term evolution. In conclusion, miRNAs may stabilize GRNs in two vastly different time scales—in developmental as well as during evolution.

Materials and Methods

Fly Stocks

The *UAS-GFP* line (w1118/Y; *miniwhite-UAS-eGFP*/*miniwhite-UAS-eGFP*) was generated by our laboratory. It is a red-eyed strain with the insertion of *mini white* and *UAS-eGFP* at 2 chromosome 51D using the PhiC31 site-specific chromosomal integration system. T98-Gal4, *UAS-Dicer-1*^{HMS00141}, and *UAS-Dicer-1* were obtained from the Bloomington stock center and are described in flybase (http://flystocks.bio.indiana.edu/), stock numbers are 6,996, 34,826, and 36,510, respectively. All flies were raised at 25 °C on a standard sugar-yeast-agar medium and under 12:12 h light/dark cycles. Heat treatment was carried out in the incubator at 30 °C for specified times.

Fly Viability Assay

Embryos were collected from 6- to 9-day-old flies, over 1–2 h on grape juice agar plates. Before embryo collection flies were kept in bottles with frequently replaced grape juice agar plates for 3 days to eliminate old eggs.

For fly viability presented in figure 4, three batches of 100–200 embryos were collected for each genotype and treatment (three genotypes × two treatments, *dcr-1* KD, wildtype and *dcr-1* rescue; 25 and 30 °C). At day 0, the number of first instar larvae (L1) was counted after 30 h, the total number of pupae and adults was counted at day 11–12. This schedule was used for flies raised at both 25 and 30 °C. Egg hatchability (embryo viability) = L1 number/egg number; larval viability = pupa number/L1 number; pupal viability (eclosion rate) = adult number/pupa number.

For pupal viability presented in figure 5, three batches of 100–200 embryos were collected for each genotype and treatment (three genotypes × seven treatments, *dcr-1* KD, wildtype and *dcr-1* rescue; 25 °C and heat pulse shown in fig. 5A, left panel). At day 0, the total number of pupae and adults (distinguishing females and males) was counted at days 11–12. Eclosion rate for female = adult female number/pupa number; Eclosion rate for male = adult male number/pupa number.

Determining Pupal Lethality Stages

To define pupal lethality stages (supplementary fig. S4, Supplementary Material online), we collected un-enclosed

pupae at day 12 for each genotype and treatment (three genotypes × two treatments: *dcr-1* KD, wildtype and *dcr-1* rescue; 25 and 30 °C). Metamorphosis of these pupae stopped at specific stages. One hundred to 200 wildtype flies were counted for each phenotype. Pupal development stages are according to Bainbridge and Bownes (1981). Briefly, pupae with yellow eyes are regarded as dead at late pupal stages, the rest at early stages; for the early pupae, pupae with legs and wings achieving full extension along the abdomen are regarded as dead at P5–P7, the rest at P1–P4. Late pupae with mature bristles on most abdomen regions are regarded as dead at P14–P15, the rest at P8–P13.

Adult Longevity Assay

Adult longevity (figs. 4 and 5) assays were performed as described in (Chen et al. 2014). Briefly, virgin females and un-mated males were collected separately, three vials (replicates) of 20 flies of each genotype and treatment (3 genotypes × 7 treatments × 2 sexes: *dcr-1* KD, wildtype and *dcr-1* rescue; 25 and 30 °C and heat pulse shown in fig. 5*A* right panel; female and male). Dead flies were counted every 2–3 days and flipped to fresh vials until all had died. Median survival was then determined and analyzed.

Detecting miRNA and Gene Expression by RT-PCR

For each genotype and treatment (3 genotypes × 2 treatments: *dcr-1* KD, wildtype and *dcr-1* rescue; 25 and 30 °C), 3 batches of 6–10 female third instar larvae (L3) were collected independently as biological replicates. L3 sex was distinguished by gonad morphology. For each replicate, total RNA was extracted using the Ambion TRIzol® Reagent (Code No. 15596018). Total RNA was reverse transcribed into cDNA using the TARAKA Mir-X miRNA First Strand Synthesis Kit (Code No. 638315) and the TOYOBO ReverTra Ace qPCR RT Master Mix with gDNA Remover (Code No. FSQ-301) for miRNA and protein-coding gene analyses, respectively. RT-PCT was performed on an ABI PRISM 7900 sequence detection system, TARAKA SYBR® Premix Ex Taq (Tli RNaseH Plus) (Code No. RR420) was used to detect amplification products. Relative expression levels were calculated as 2^{-ddct}. Primers used in this study are shown in supplementary table S2, Supplementary Material online. We used *rp49* as internal reference control for protein-coding genes. We used uridine-rich 6 (U6) small nuclear RNA as internal reference for miRNAs. U6 is one of the most widely used endogenous control for measuring the expression change of miRNAs (Sun et al. 2004; Luo et al. 2018; Gabisonia et al. 2019). We (Liufu et al. 2017; Ma et al. 2020) and other groups (Schweisgut et al. 2017; Luo et al. 2018) have independently used *U6* as the endogenous control of miRNA qRT-PCR assay.

Small RNA-Seq Analyses and Target Site Prediction

Small RNA libraries of L3 were retrieved from GEO (Gene Expression Omnibus) with accessions GSM322208 and GSM322245. High confidence miRNA precursors and mature sequences were retrieved from miRBase Release 21 (http://www.mirbase.org; Kozomara and Griffiths-Jones 2014). *Drosophila melanogaster* genome and 3′-UTR sequences (r6.04) were retrieved from FlyBase (http://flybase.org/; Attrill et al. 2016). The expression of each mature miRNA was measured using miRDeep2 version 2.0.0.7 (Friedlander et al. 2012) with default parameters, normalized by total reads matching all miRNA precursors per library and scaled as reads per million. miRNA targets were predicted using TargetScan Fly version 7.2 (Agarwal et al. 2018). Conserved miRNA targets were predicted by TargetScan based on conservation with PCT score >0.8. The PTC score reflected the probability that a site is conserved due to selective maintenance of miRNA targeting rather than by chance or any other reason not pertinent to miRNA targeting (Friedman et al. 2009). This cutoff has been used in previous publications for choosing conserved miRNA targets (Lu and Clark 2012; Ma et al. 2020).

RNA-Seq Analyses of TFs KD

To select typical TFs for analysis, we obtained curated list of TFs at the DRSC (http://www.flyrnai.org/supplement/TranscriptionFactorGenes.xls). TFs list were filtered by requiring they (1) have experimental evidence of TF activity and DNA binding; (2) have public RNA-seq data of RNAi-mediated knockdown in S2R+ cells (https://www.ncbi.nlm.nih.gov/geo/query/acc.cgi?acc=GSE89753). This gave a list of 42 TFs across 18 TF families. For each of the 18 TF gene families, gene with the lowest correlation between the gene expression profile (GEO ID: GSE89753) of the wildtype and that of the TF knocking down cells was selected and presented in table 1.

RNA-Seq Analyses of *dcr-1* KD Lines

Total RNA was extracted from ∼10 larvae using the TRIzol® Reagent, ribo-depleted total-RNA libraries were constructed and sequenced on Illumina HiSeq 2000 at BGI (http://www.genomics.cn/index). *Drosophila melanogaster* genome (BDGP6.83) was retrieved from the Ensembl database. RNA-seq reads were mapped to the *D. melanogaster* reference genome using Tophat (v2.1.0). The number of reads mapping to each protein-coding gene were quantified using HTseq (v0.6.0). Significantly dysregulated genes were called using DEseq2 (Love et al. 2014) with $FDR < 0.1$. Similar to previous work (Yeh et al. 2014), a Generalized Linear Model was used to calculate the impact of each factor (sex, temperature, and genotype) on gene expression using the DESeqDataSet object:

$$y_{ijl} = \mu + S_i + T_j + G_l + \varepsilon_{ijl}$$

In this formula, y_{ijl} refers gene expression for the ith sex, jth temperature, lth genotype; μ is the baseline expression, S_i is the effect of the ith sex, T_j is the effect of the jth temperature, G_l is the effect of the lth genotype, ϵ is the error term.

To define the genes affected by genotype (*dcr-1*KD), temperature, genotype × environment interactions for each sex, the following Generalized Linear Model was used:

$$y_{jl} = \mu + T_j + G_l + T_jG_l + \varepsilon_{jl}$$

In this formula, y_{jl} refers gene expression for the jth temperature, lth genotype; μ is the baseline expression, T_j is the effect of the jth temperature, G_l is the effect of the lth genotype, T_jG_l is the interaction term, ϵ is the error term.

Significantly dysregulated genes affected by each factor were called with the $FDR < 0.1$ cutoff. To quantify gene expression and remove the dependence of variance on the mean, the function *vst* (variance stabilizing transformations) in DESeq2 was used to transform gene count data. Genes with read coverage <4 were not included in our analysis. GO enrichment was estimated using David 6.8 (Huang et al. 2009) with cutoff *P*–value 0.01.

Supplementary Material

Supplementary data are available at *Molecular Biology and Evolution* online.

Acknowledgments

The authors thank all members in the Wu laboratory for helpful comments and sharing of ideas. They thank Suhua Shi, Xu Shen, Yongsen Ruan, Mei Hou, Jianguo Wang, Kehui Liu, and Yumei Huang, Sun Yat-sen University, for extensive discussions and critical reading of the manuscript. They thank Hurng-Yi Wang, National Taiwan University, and Xuan Guo, Jinzhou Medical University, for generous help in shipping Drosophila stocks. G.A.L. acknowledges the Society for Molecular Biology & Evolution for providing travel award to attend the 2019 SMBE meeting, and the support of Treasurer Jeff Thorne, North Carolina State University, and Christopher Lapine, Allen Press, during the travel award reimbursement process. This work was supported by National Natural Science Foundation of China (31900417, 32293193, 31801081, 31730046, 81972691, and 31970245), Guangdong Basic and Applied Basic Research Foundation (2019A1515010708, 2020A1515010467, and 2020B1515020030), China Postdoctoral Science Foundation (2020T130748), Guangdong Key Research and Development Program (2022B1111030001), Innovation Group Project of Southern Marine Science and Engineering Guangdong Laboratory (Zhuhai) (311021006).

Author Contributions

G.A.L., Z.L., T.T., H.W., and C.I.W. conceived and designed the study. G.A.L., J.Z., Y.Z., and Q.C. performed analyses with assistance from Z.T., and P.L., C.I.W., G.A.L., and Y.Z wrote the paper, with critical revisions provided by all authors.

Data Availability

All raw RNA sequencing data were submitted to the National Genomics Data Center (https://bigd.big.ac.cn/) with accession number PRJCA006274. The open software used in this study is cited and materials can be requested from the authors.

Conflict of interest statement. The authors declare that they have no competing interests.

References

Agarwal V, Subtelny AO, Thiru P, Ulitsky I, Bartel DP. 2018. Predicting microRNA targeting efficacy in Drosophila. *Genome Biol*. **19**:152.

Ambros V. 2019. Mathematics of microRNAs: stabilizing gene regulatory networks. *Natl Sci Rev*. **6**:1189–1190.

Ambros V, Ruvkun G. 2018. Recent molecular genetic explorations of *Caenorhabditis elegans* microRNAs. *Genetics* **209**:651–673.

Attrill H, Falls K, Goodman JL, Millburn GH, Antonazzo G, Rey AJ, Marygold SJ, FlyBase C. 2016. FlyBase: establishing a gene group resource for *Drosophila melanogaster*. *Nucleic Acids Res*. **44**: D786–D792.

Bainbridge SP, Bownes M. 1981. Staging the metamorphosis of *Drosophila melanogaster*. *Development* **66**:57–80.

Bartel DP. 2018. Metazoan microRNAs. *Cell* **173**:20–51.

Cassidy JJ, Jha AR, Posadas DM, Giri R, Venken KJT, Ji J, Jiang H, Bellen HJ, White KP, Carthew RW. 2013. miR-9a minimizes the phenotypic impact of genomic diversity by buffering a transcription factor. *Cell* **155**:1556–1567.

Chen J, Nolte V, Schlotterer C. 2015. Temperature-related reaction norms of gene expression: regulatory architecture and functional implications. *Mol Biol Evol*. **32**:2393–2402.

Chen Y, Shen Y, Lin P, Tong D, Zhao Y, Allesina S, Shen X, Wu CI. 2019. Gene regulatory network stabilized by pervasive weak repressions: microRNA functions revealed by the May–Wigner theory. *Natl Sci Rev*. **6**:1176–1188.

Chen YW, Song S, Weng R, Verma P, Kugler JM, Buescher M, Rouam S, Cohen S. 2014. Systematic study of *Drosophila* microRNA functions using a collection of targeted knockout mutations. *Dev Cell*. **31**:784–800.

Chen Q, Yang H, Feng X, Chen Q, Shi S, Wu CI, He Z. 2022. Two decades of suspect evidence for adaptive molecular evolution-negative selection confounding positive-selection signals. *Natl Sci Rev*. **9**:nwab217.

Ebert MS, Sharp PA. 2012. Roles for microRNAs in conferring robustness to biological processes. *Cell* **149**:515–524.

Eichhorn SW, Guo H, McGeary SE, Rodriguez-Mias RA, Shin C, Baek D, Hsu SH, Ghoshal K, Villén J, Bartel DP. 2014. mRNA destabilization is the dominant effect of mammalian microRNAs by the time substantial repression ensues. *Mol Cell*. **56**:104–115.

Farh KK, Grimson A, Jan CH, Lewis BP, Johnston WK, Lim LP, Burge CB, Bartel DP. 2005. The widespread impact of mammalian microRNAs on mRNA repression and evolution. *Science* **310**: 1817–1821.

Félix MA, Barkoulas M. 2015. Pervasive robustness in biological systems. *Nat Rev Genet*. **16**:483–496.

Friedlander MR, Mackowiak SD, Li N, Chen W, Rajewsky N. 2012. miRDeep2 accurately identifies known and hundreds of novel microRNA genes in seven animal clades. *Nucleic Acids Res*. **40**: 37–52.

Friedman RC, Farh KK, Burge CB, Bartel DP. 2009. Most mammalian mRNAs are conserved targets of microRNAs. *Genome Res*. **19**: 92–105.

Gabisonia K, Prosdocimo G, Aquaro GD, Carlucci L, Zentilin L, Secco I, Ali H, Braga L, Gorgodze N, Bernini F, *et al.* 2019. MicroRNA therapy stimulates uncontrolled cardiac repair after myocardial infarction in pigs. *Nature* **569**:418–422.

Galagali H, Kim JK. 2020. The multifaceted roles of microRNAs in differentiation. *Curr Opin Cell Biol*. **67**:118–140.
Guo Y, Amir A. 2021. Exploring the effect of network topology, mRNA and protein dynamics on gene regulatory network stability. *Nat Commun*. **12**:130.
Hallgrimsson B, Green RM, Katz DC, Fish JL, Bernier FP, Roseman CC, Young NM, Cheverud JM, Marcucio RS. 2019. The developmental-genetics of canalization. *Semin Cell Dev Biol*. **88**: 67–79.
Hintze M, Katsanos D, Shahrezaei V, Barkoulas M. 2021. Phenotypic robustness of epidermal stem cell number in *C. elegans* is modulated by the activity of the conserved N-acetyltransferase nath-10/NAT10. *Front Cell Dev Biol*. **9**:640856.
Hrdlicka L, Gibson M, Kiger A, Micchelli C, Schober M, Schock F, Perrimon N. 2002. Analysis of twenty-four Gal4 lines in *Drosophila melanogaster*. *Genesis* **34**:51–57.
Huang DW, Sherman BT, Lempicki RA. 2009. Systematic and integrative analysis of large gene lists using DAVID bioinformatics resources. *Nat Protoc*. **4**:44–57.
Jiang N, Soba P, Parker E, Kim CC, Parrish JZ. 2014. The microRNA bantam regulates a developmental transition in epithelial cells that restricts sensory dendrite growth. *Development* **141**:2657–2668.
Kasper DM, Moro A, Ristori E, Narayanan A, Hill-Teran G, Fleming E, Moreno-Mateos M, Vejnar CE, Jing Z, Lee D. 2017. MicroRNAs establish uniform traits during the architecture of vertebrate embryos. *Dev Cell*. **40**:552–565.e555.
Kozomara A, Birgaoanu M, Griffiths-Jones S. 2019. miRBase: from microRNA sequences to function. *Nucleic Acids Res*. **47**: D155–D162.
Kozomara A, Griffiths-Jones S. 2014. miRBase: annotating high confidence microRNAs using deep sequencing data. *Nucleic Acids Res*. **42**:D68–D73.
Lee RC, Feinbaum RL, Ambros V. 1993. The *C. elegans* heterochronic gene lin-4 encodes small RNAs with antisense complementarity to lin-14. *Cell* **75**:843–854.
Levy SF, Siegal ML. 2008. Network hubs buffer environmental variation in *Saccharomyces cerevisiae*. *PLoS Biol*. **6**:e264.
Li X, Cassidy JJ, Reinke CA, Fischboeck S, Carthew RW. 2009. A microRNA imparts robustness against environmental fluctuation during development. *Cell* **137**:273–282.
Lin P, Lu GA, Liufu Z, Zhao YX, Ruan Y, Wu CI, Wen H. 2022. Gene expression as phenotype—many small-step changes leading to little long-term phenotypic evolution. *bioRxiv*. https://10.1101/2022.06.24.497468.
Liufu Z, Zhao Y, Guo L, Miao G, Xiao J, Lyu Y, Chen Y, Shi S, Tang T, Wu CI. 2017. Redundant and incoherent regulations of multiple phenotypes suggest microRNAs' role in stability control. *Genome Res*. **27**:1665–1673.
Love MI, Huber W, Anders S. 2014. Moderated estimation of fold change and dispersion for RNA-seq data with DESeq2. *Genome Biol*. **15**:550–550.
Lu J, Clark AG. 2012. Impact of microRNA regulation on variation in human gene expression. *Genome Res*. **22**:1243–1254.
Lu J, Shen Y, Wu Q, Kumar S, He B, Shi S, Carthew RW, Wang SM, Wu CI. 2008. The birth and death of microRNA genes in *Drosophila*. *Nat Genet*. **40**:351–355.
Lu GA, Zhao Y, Yang H, Lan A, Shi S, Liufu Z, Huang Y, Tang T, Xu J, Shen X, *et al.* 2018. Death of new microRNA genes in *Drosophila* via gradual loss of fitness advantages. *Genome Res*. **28**:1309–1318.
Ludwig N, Leidinger P, Becker K, Backes C, Fehlmann T, Pallasch C, Rheinheimer S, Meder B, Stähler C, Meese E, *et al.* 2016. Distribution of miRNA expression across human tissues. *Nucleic Acids Res*. **44**:3865–3877.
Luo M, Gao Z, Li H, Li Q, Zhang C, Xu W, Song S, Ma C, Wang S. 2018. Selection of reference genes for miRNA qRT-PCR under abiotic stress in grapevine. *Sci Rep*. **8**:4444.
Lyu Y, Shen Y, Li H, Chen Y, Guo L, Zhao Y, Hungate E, Shi S, Wu CI, Tang T. 2014. New microRNAs in Drosophila—birth, death and cycles of adaptive evolution. *PLoS Genet*. **10**:229–231.
Ma F, Lu GA, Chen Q, Ruan Y, Li X, Lu X, Li C. 2020. Dynamic global analysis of transcription reveals the role of miRNAs in synergistic stabilization of gene expression. *Sci Bull*. **65**:2130–2140.
May RM. 1972. Will a large complex system be stable? *Nature* **238**: 413–414.
May RM. 1974. *Stability and complexity in model ecosystems*. Princeton: Princeton University Press.
Nagosa S, Leesch F, Putin D, Bhattacharya S, Altshuler A, Serror L, Amitai-Lange A, Nasser W, Aberdam E, Rouleau M, *et al.* 2017. microRNA-184 induces a commitment switch to epidermal differentiation. *Stem Cell Reports* **9**:1991–2004.
Ni JQ, Zhou R, Czech B, Liu LP, Holderbaum L, Yang-Zhou D, Shim HS, Tao R, Handler D, Karpowicz P, *et al.* 2011. A genome-scale shRNA resource for transgenic RNAi in *Drosophila*. *Nat Methods*. **8**:405–407.
Nozawa M, Miura S, Nei M. 2012. Origins and evolution of microRNA genes in plant species. *Genome Biol Evol*. **4**:230–239.
Peláez N, Carthew RW. 2012. Biological robustness and the role of microRNAs: a network perspective. *Curr Top Dev Biol*. **99**: 237–255.
Posadas DM, Carthew RW. 2014. MicroRNAs and their roles in developmental canalization. *Curr Opin Genet Dev*. **27**:1–6.
Rahmanian S, Murad R, Breschi A, Zeng W, Mackiewicz M, Williams B, Davis CA, Roberts B, Meadows S, Moore D, *et al.* 2019. Dynamics of microRNA expression during mouse prenatal development. *Genome Res*. **29**:1900–1909.
Rendel JM. 1967. *Canalisation and gene control*. London: Logos Press.
Rutherford SL, Lindquist S. 1998. Hsp90 as a capacitor for morphological evolution. *Nature* **396**:336–342.
Saiz N, Mora-Bitria L, Rahman S, George H, Herder JP, Garcia-Ojalvo J, Hadjantonakis AK. 2020. Growth-factor-mediated coupling between lineage size and cell fate choice underlies robustness of mammalian development. *Elife* **9**:e56079.
Scharloo W. 1991. Canalization: genetic and developmental aspects. *Annu Rev Ecol Syst*. **22**:65–93.
Schmiedel JM, Klemm SL, Zheng Y, Sahay A, Blüthgen N, Marks DS, van Oudenaarden A. 2015. Gene expression. MicroRNA control of protein expression noise. *Science* **348**:128–132.
Schweisgut J, Schutt C, Wüst S, Wietelmann A, Ghesquière B, Carmeliet P, Dröse S, Korach KS, Braun T, Boettger T. 2017. Sex-specific, reciprocal regulation of ERα and miR-22 controls muscle lipid metabolism in male mice. *EMBO J*. **36**:1199–1214.
Seitz H. 2019. On the number of functional microRNA targets. *Mol Biol Evol*. **36**:1596–1597.
Sgro CM, Terblanche JS, Hoffmann AA. 2016. What can plasticity contribute to insect responses to climate change. *Annu Rev Entomol*. **61**:433–451.
Siciliano V, Garzilli I, Fracassi C, Criscuolo S, Bernardo DD. 2013. miRNAs confer phenotypic robustness to gene networks by suppressing biological noise. *Nat Commun*. **4**:2364.
Siegal ML, Leu JY. 2014. On the nature and evolutionary impact of phenotypic robustness mechanisms. *Annu Rev Ecol Evol Syst*. **45**:496–517.
Sun Y, Koo S, White N, Peralta E, Esau C, Dean NM, Perera RJ. 2004. Development of a micro-array to detect human and mouse microRNAs and characterization of expression in human organs. *Nucleic Acids Res*. **32**:e188.
Takahashi KH. 2019. Multiple modes of canalization: links between genetic, environmental canalizations and developmental stability, and their trait-specificity. *Semin Cell Dev Biol*. **88**:14–20.
Vihervaara A, Duarte FM, Lis JT. 2018. Molecular mechanisms driving transcriptional stress responses. *Nat Rev Genet*. **19**:385–397.
Waddington CH. 1942. Canalization of development and the inheritance of acquired characters. *Nature* **150**:563–565.
Waddington CH. 1957. *The strategy of the genes*. London: Allen and Unwin.
Waddington CH. 1959. Canalization of development and genetic assimilation of acquired characters. *Nature* **183**:1654–1655.
Wagner A. 2005. *Robustness and evolvability in living systems*. Princeton: Princeton University Press.

Wei L, Li S, Zhang P, Hu T, Zhang MQ, Xie Z, Wang X. 2021. Characterizing microRNA-mediated modulation of gene expression noise and its effect on synthetic gene circuits. *Cell Rep*. **36**: 109573.

Wen HJ, Liu FL, Huang MX, Luo RH, He WB, Feng J, Chen FL, Cai QC, Ma HJ, Yang ZF, *et al.* 2021. A proposal for clinical trials of COVID-19 treatment using homo-harringtonine. *Natl Sci Rev*. **8**:nwaa257.

Wu CI, Shen Y, Tang T. 2009. Evolution under canalization and the dual roles of microRNAs: a hypothesis. *Genome Res*. **19**:734–743.

Xu J, Zhang R, Shen Y, Liu G, Lu X, Wu CI. 2013. The evolution of evolvability in microRNA target sites in vertebrates. *Genome Res*. **23**: 1810–1816.

Yeh SD, Grotthuss MV, Gandasetiawan KA, Jayasekera S, Xia XQ, Chan C, Jayaswal V, Ranz JM. 2014. Functional divergence of the miRNA transcriptome at the onset of Drosophila metamorphosis. *Mol Biol Evol*. **31**:2557.

Zhao Y, Lin P, Liufu Z, Yang H, Lyu Y, Shen X, Wu CI, Tang T. 2018. Regulation of large number of weak targets-new insights from twin-microRNAs. *Genome Biol Evol*. **10**:1255–1264.

Zhao Y, Lu GA, Yang H, Lin P, Liufu Z, Tang T, Xu J. 2021. Run or die in the evolution of new microRNAs-testing the red queen hypothesis on de novo new genes. *Mol Biol Evol*. **38**:1544–1553.

Zhao Y, Shen X, Tang T, Wu CI. 2017. Weak regulation of many targets is cumulatively powerful—an evolutionary perspective on microRNA functionality. *Mol Biol Evol*. **34**:3041–3046.

Zhao Y, Shen X, Tang T, Wu C. 2019. Weak regulation of many targets is cumulatively powerful—a reply to Seitz on microRNA functionality. *Mol Biol Evol*. **36**:1598–1599.